Picosecond and nanosecond pulse delivery through a hollow-core Negative Curvature Fiber for micro-machining applications

Piotr Jaworski,[1*] Fei Yu,[2] Robert R.J. Maier,[1] William J. Wadsworth,[2] Jonathan C. Knight,[2] Jonathan D. Shephard,[1] and Duncan P. Hand[1]

[1]*Applied Optics and Photonics Group, Institute of Photonics and Quantum Sciences, Heriot-Watt University, Edinburg, EH14 4AS, UK*

[2] *Centre for Photonics and Photonic Materials, Department of Physics, University of Bath, Bath, BA2 7AY, UK*

**pj46@hw.ac.uk*

Abstract: We present high average power picosecond and nanosecond pulse delivery at 1030 nm and 1064 nm wavelengths respectively through a novel hollow-core Negative Curvature Fiber (NCF) for high-precision micro-machining applications. Picosecond pulses with an average power above 36 W and energies of 92 μJ, corresponding to a peak power density of 1.5 TWcm^{-2} have been transmitted through the fiber without introducing any damage to the input and output fiber end-faces. High-energy nanosecond pulses (>1 mJ), which are ideal for micro-machining have been successfully delivered through the NCF with a coupling efficiency of 92%. Picosecond and nanosecond pulse delivery have been demonstrated in fiber-based laser micro-machining of fused silica, aluminum and titanium.

OCIS codes: (060.0060) Fiber optics and optical communications; (060.2270) Fiber characterization; (060.5295) Photonic crystal fibers; (350.3390) Laser materials processing.

References and Links

1. J. D. Shephard, J. D. C. Jones, D. P. Hand, G. Bouwmans, J. C. Knight, P. St. J. Russell, and B. J. Mangan, "High energy nanosecond laser pulses delivered single-mode through hollow-core PBG fibers," Opt. Express **12**(4), 717–723 (2004).
2. S. Fevrier, D. Gruppi, P. Viale, C. Humbert, R. Jamier, B. Beadou, A. Hirth, S. L. Semjonov, M. E. Likhachev, M. M. Bubnov, E. M. Dianov, V. F. Khopin, M. Y. Salganskii, and A. N. Guryanov, "High-energy nanosecond pulse delivery through singlemode large mode area all-solid bandgap fibers," presented at European Conference on Optical Communications (ECOC), Cannes, 24–28 Sept. 2006.
3. A. Kuhn, P. French, D. P. Hand, I. J. Blewett, M. Richmond, and J. D. C. Jones, "Preparation of fiber optics for the delivery of high-energy high-beam-quality Nd:YAG laser pulses," Appl. Opt. **39**(33), 6136–6143 (2000).
4. D. Su, A. A. B. Boechat, and J. D. C. Jones, "Optimum beam launching conditions for graded-index optical fibers - theory and practice," IEEE Proc. J **140**, 221–226 (1993).
5. A. Kuhn, I. J. Blewett, D. P. Hand, P. French, M. Richmond, and J. D. C. Jones, "Optical fibre beam delivery of high-energy laser pulses: beam quality preservation and fibre end-preparation," Opt. Lasers Eng. **34**(4-6), 273–288 (2000).
6. J. P. Parry, T. J. Stephens, J. D. Shephard, J. D. C. Jones, and D. P. Hand, "Analysis of optical damage mechanisms in hollow-core waveguides delivering nanosecond pulses from a Q-switched Nd:YAG laser," Appl. Opt. **45**(36), 9160–9167 (2006).
7. G. P. Agrawal, *Nonlinear Fiber Optics* (Academic, 2001).
8. N. A. Issa, A. Argyros, M. A. van Eijkelenborg, and J. Zagari, "Identifying hollow waveguide guidance in air-cored microstructured optical fibres," Opt. Express **11**(9), 996–1001 (2003).
9. A. Urich, R. R. J. Maier, B. J. Mangan, S. Renshaw, J. C. Knight, D. P. Hand, and J. D. Shephard, "Delivery of high energy Er:YAG pulsed laser light at 2.94 μm through a silica hollow core photonic crystal fibre," Opt. Express **20**(6), 6677–6684 (2012).
10. B. Beaudou, F. Gerôme, Y. Y. Wang, M. Alharbi, T. D. Bradley, G. Humbert, J.-L. Auguste, J.-M. Blondy, and F. Benabid, "Millijoule laser pulse delivery for spark ignition through kagome hollow-core fiber," Opt. Lett. **37**(9), 1430–1432 (2012).
11. F. Emaury, C. F. Dutin, C. J. Saraceno, M. Trant, O. H. Heckl, Y. Y. Wang, C. Schriber, F. Gerome, T. Südmeyer, F. Benabid, and U. Keller, "Beam delivery and pulse compression to sub-50 fs of a modelocked thin-disk laser in a gas-filled Kagome-type HC-PCF fiber," Opt. Express **21**(4), 4986–4994 (2013).

#191496 - $15.00 USD Received 12 Jun 2013; revised 7 Sep 2013; accepted 9 Sep 2013; published 19 Sep 2013

12. F. Yu, W. J. Wadsworth, and J. C. Knight, "Low loss silica hollow core fibers for 3-4 μm spectral region," Opt. Express **20**(10), 11153–11158 (2012).
13. A. D. Pryamikov, A. S. Biriukov, A. F. Kosolapov, V. G. Plotnichenko, S. L. Semjonov, and E. M. Dianov, "Demonstration of a waveguide regime for a silica hollow--core microstructured optical fiber with a negative curvature of the core boundary in the spectral region > 3.5 μm," Opt. Express **19**(2), 1441–1448 (2011).
14. A. Urich, R. R. J. Maier, F. Yu, J. C. Knight, D. P. Hand, and J. D. Shephard, "Flexible delivery of Er:YAG radiation at 2.94 μm with negative curvature silica glass fibers: a new solution for minimally invasive surgical procedures," Biomed. Opt. Express **4**(2), 193–205 (2013).
15. N. M. Litchinitser, A. K. Abeeluck, C. Headley, and B. J. Eggleton, "Antiresonant reflecting photonic crystal optical waveguides," Opt. Lett. **27**(18), 1592–1594 (2002).
16. J. D. Shephard, F. Couny, P. St. J. Russell, J. D. C. Jones, J. C. Knight, and D. P. Hand, "Improved hollow-core photonic crystal fiber design for delivery of nanosecond pulses in laser micromachining applications," Appl. Opt. **44**(21), 4582–4588 (2005).
17. G. Mann, J. Vogel, R. Preuss, P. Vaziri, M. Zoheidi, M. Eberstein, and J. Kruger, "Nanosecond laser-induced surface damage of optical multimode fibers and their preforms," Appl. Opt. A **92**, 853–857 (2008).

1. Introduction

High average power short pulsed lasers are increasingly used for micromachining. However flexible fiber beam delivery systems for such lasers are limited in terms of pulse energy, restricting the range of potential applications. As a result, these lasers are typically used to process flat parts placed under a galvo scan head. A suitable fiber delivery system is hence important to extend applications to the processing of complex 3D components.

Results obtained over the last couple of years have demonstrated the suitability of hollow-core photonic crystal fibers (HC-PCFs), hollow waveguides and large mode area solid core fibers for high-energy pulse delivery [1–6]. These fibers overcome limitations due to the low damage threshold and nonlinear effects dominant in conventional single-mode solid core silica fibers [7,8] and can also minimize attenuation imposed by material absorption [9]. However their energy handling capability is still limited to approximately 1 mJ in the ns pulse regime and efficient delivery of high energy ps pulses was not reported.

In 2012 Benabid et al reported a new design of kagome-type hollow-core microstructured fiber [10] with a hypocycloid shaped core (negative curvature), capable of delivering ns pulses with energies in the range of 10 mJ. Moreover their latest work presents delivery of 10.5 ps pulses with an energy of approximately 97 μJ and an average power of 5 W, corresponding to a peak power of 8 MW through 10 cm long kagome fiber [11]. These reported fibers however have a complicated structure, which requires stacking many layers of capillaries during preform fabrication. Consequently a less complex design which still provided the negative curvature of the core wall, the so called Negative Curvature Fiber (NCF), was presented in [12,13]. This fiber proved to be a great candidate for high-power delivery of Er:YAG laser pulses at a wavelength of 2.94 μm for medical applications [14].

In this paper we investigate a similar hollow-core Negative Curvature Fiber optimized for the delivery of high-power, high-energy ns and ps pulses in the 1 μm wavelength region for precision micro-machining applications.

2. Negative Curvature Fiber (NCF)

2.1 Fiber structure and light guidance mechanism

The NCF was fabricated by the commonly used stack and draw technique, described in [12]. Eight identical circular capillaries were used to form a preform, which was drawn down to produce a final fiber with 43 μm diameter hollow air core and NA of 0.03 (measured) as shown in Fig. 1(a). To shape the negative curvature structure different pressures were applied to the core and the cladding during the fiber drawing process (details of fiber fabrication are given in [12]). The crucial points of the fiber are cladding nodes between adjacent capillaries, marked with red circles in Fig. 1(b), which introduce high losses. These nodes behave as independent waveguides supporting their own lossy modes. Therefore, the curvature of the cladding (core wall) is directed in the opposite direction (in comparison with a typical cylindrical core such as in the HC-PCF structure) in order to physically separate the fiber guided mode from the cladding nodes, significantly reducing coupling between them.

#191496 - $15.00 USD Received 12 Jun 2013; revised 7 Sep 2013; accepted 9 Sep 2013; published 19 Sep 2013

The light guidance mechanism in the NCF is based on the Anti-Resonant Reflecting Optical Waveguiding (ARROW) phenomenon, which means that its structure can behave as a Fabry-Perot resonant cavity [15]. Therefore all wavelengths of light which are not in resonance with the core wall are reflected back into the core and propagate with low loss as a result of destructive interference in the Fabry-Perot resonator. The resonant frequencies, meanwhile, cannot be confined in the core and leak away to the cladding region where they are highly attenuated. The wavelengths that are guided are hence strongly dependent on the thickness of the core wall (capillaries); for guidance at 1030 nm and 1064 nm a suitable wall thickness is in the range of 910 ± 50 nm.

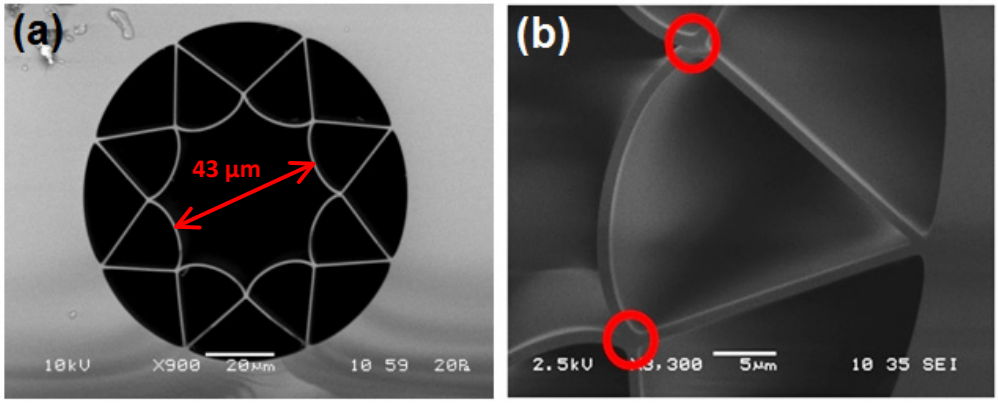

Fig. 1. (a) SEM image of the NCF used in the experiments. (b) SEM picture of the capillary forming the negative curvature of the fiber core wall.

2.2 Fiber attenuation

To measure the attenuation of the NCF at 1030 nm and 1064 nm wavelengths a cutback technique was used. With this fiber a high bending sensitivity was observed (further investigation of this phenomenon is described in section 2.3), therefore, to measure attenuation independently of bend loss a 1 m long, straight fiber was used. Any additional micro-bends, which could potentially affect the results, were minimized by maintaining the fiber within the same horizontal position during the entire experiment.

A TRUMPF TruMicro ps laser (M^2~1.3) and a JDS Uniphase microchip ns laser (M^2~1.2) were used as coherent light sources for 1030 nm and 1064 nm wavelengths respectively. In both cases the fiber was cut from 1 m to 10 cm while maintaining the same coupling conditions. The fiber attenuation was measured to be at the level of 0.23 dB/m and 0.16 dB/m for 1030 nm and 1064 nm respectively.

To obtain a loss spectrum over a wide spectral range from 1000 nm to 1400 nm (in this case with a coiled fiber) and determine the antiresonant bandwidth position, an additional cutback measurement was carried out with a broadband light source (a tungsten halogen bulb). The FC-connectorized fiber was connected to an Ando Optical Spectrum Analyzer AQ-6315B. In this case the fiber was cutback from 87 m to 3 m. The low-loss region covers over 300 nm (1000 nm –1330 nm) of the IR spectral bandwidth. The attenuation spectrum of the NCF is presented in Fig. 2.

#191496 - $15.00 USD Received 12 Jun 2013; revised 7 Sep 2013; accepted 9 Sep 2013; published 19 Sep 2013

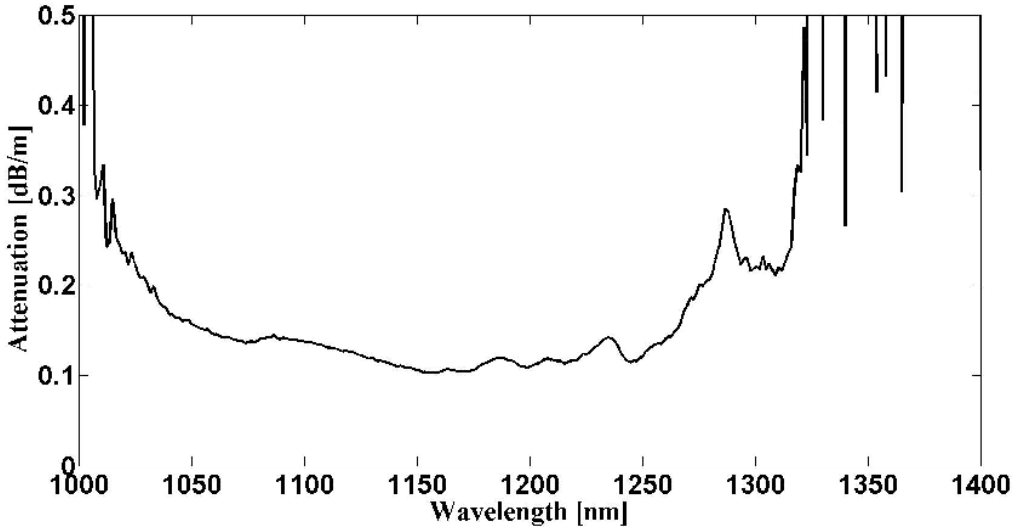

Fig. 2. Attenuation spectrum of the NCF.

2.3 Bending losses

The fabricated NCF is sensitive to bending or any applied physical force e.g. point load, which introduce additional, significant losses. To fully understand the bending loss mechanism of the fiber, a series of different tests were performed. The measurements were conducted at 1064 nm with a JDS Uniphase microchip ns laser.

The bending losses were measured for both a coiled fiber (4.1 m long) and with a 180° bend (3.1 m long) fiber. In both cases, the launching side of the fiber and its bent part were kept in the same horizontal plane to avoid micro-bends. Moreover, to maintain the same coupling conditions for each measurement the input end-face of the fiber was not moved during the entire experiment.

The results plotted in Figs. 3 and 5 demonstrate that fiber bending has a significant impact on the light delivered for bending diameters below 40 cm (2.5 coils) and 25 cm for coiled and 180° bent fiber respectively. For larger bend radii, no bend-induced loss was detected. In addition, changes in the delivered mode patterns were observed by imaging the fiber output with a CCD camera during fiber bending as shown in Figs. 4 and 6. In the case of coiling the fiber the delivered beam patterns are more single-mode like in comparison with a single 180° bend, which indicates significant attenuation of the higher order modes along the longer bending lengths. Observed fiber output beam profiles are not specific to a particular bend diameters but are representative of various profiles which can be visible at any bend radius. It is likely that the observed excitation of the different modes during fiber bending is easy to induce mainly due to very similar propagation constant of the higher order modes and the fundamental mode which results in coupling between them. Moreover, coupling between guided modes can be induced by applying a point force to either a straight or bent fiber (i.e. touching or moving it). As a result the delivered power can vary by up to ± 10%. However, when the fiber is stationary no changes in the delivered beam profile and power can be observed.

#191496 - $15.00 USD Received 12 Jun 2013; revised 7 Sep 2013; accepted 9 Sep 2013; published 19 Sep 2013

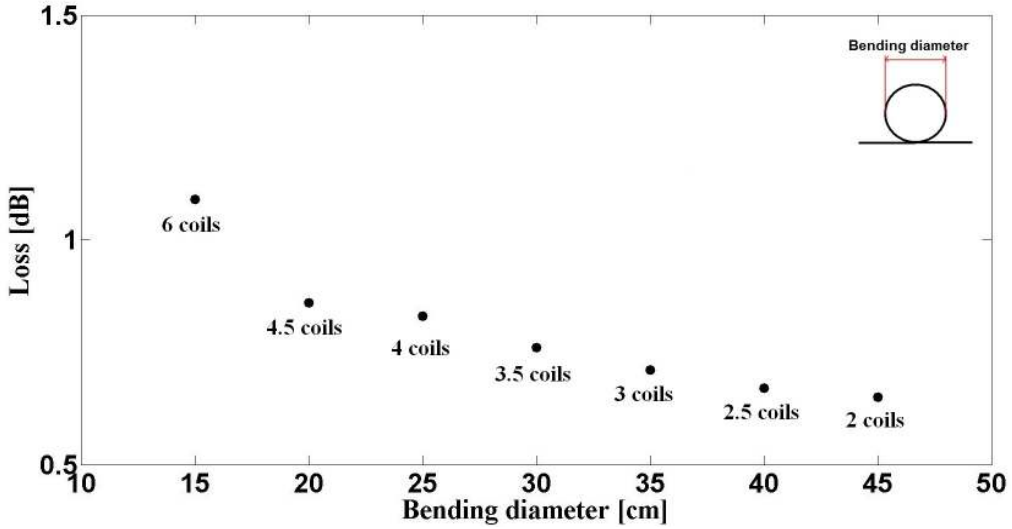

Fig. 3. Overall loss in 4.1 m long NCF due to fiber attenuation and coiling.

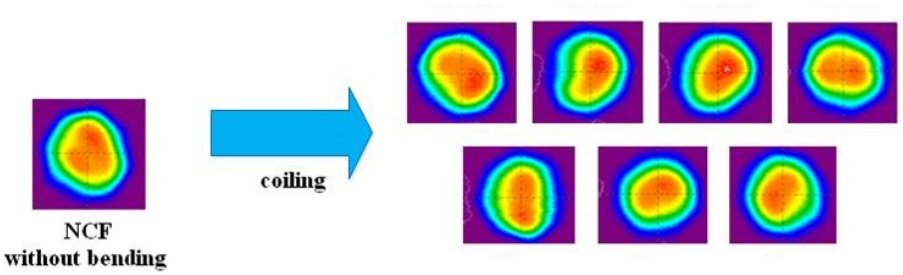

Fig. 4. Different fiber-delivered near-field beam profiles for different diameter fiber coils.

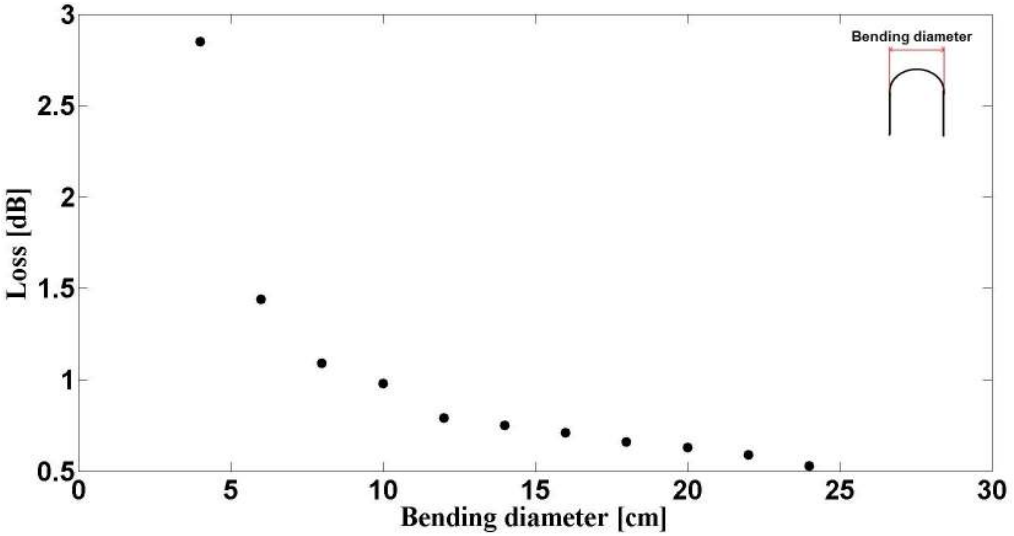

Fig. 5. Overall loss in 3.1 m long NCF introduced by fiber attenuation and 180° bend.

#191496 - $15.00 USD Received 12 Jun 2013; revised 7 Sep 2013; accepted 9 Sep 2013; published 19 Sep 2013

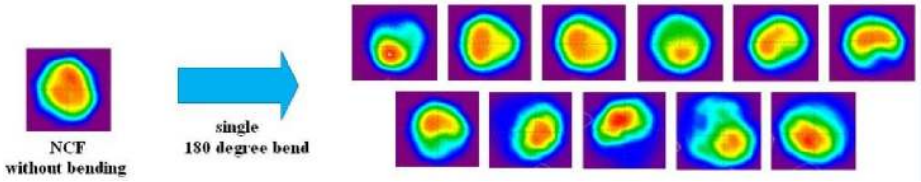

Fig. 6. Different fiber-delivered near-field beam profiles associated with single 180° bend.

3. High power pulse delivery

3.1 Damage limitation of the NCF

The laser damage threshold of the NCF was investigated with ps and ns lasers. In both cases a singlet lens (of different focal length for each laser) giving a focused spot diameter of ~36 μm ($1/e^2$) with a focus cone angle of 0.029 rad and 0.09 rad for ps and ns lasers respectively was used to couple the laser beam into the fiber with high launch efficiency. The coupling efficiency was at the level of 84% and 78% for the ps and ns lasers respectively. In the case of the ns laser, a high coupling efficiency was obtained mainly due to multimode guidance of the fiber.

The available industrial TRUMPF TruMicro ps laser (M^2~1.3) provided 6 ps pulses with a maximum average power of 46.3 W and pulse energies of 116 μJ at 1030 nm, corresponding to a peak power of 19.3 MW and a peak power density at the fiber launch of 1.75 $TWcm^{-2}$. Even at this maximum power level, the fiber did not suffer any damage, so it was impossible to establish the damage limitation of the NCF. The coupled peak power was two times greater than the critical value for a hypocycloid kagome hollow-core fiber reported in [11]. The coupling efficiency was 84%, providing a delivered pulse energy of 92 μJ through 1 m of fiber. The fiber was also tested using a Q-switched ns laser (M^2~5-6) with a pulse width of 9 ns and repetition rate of 10 Hz at 1064 nm. The input pulse energy was gradually increased until fiber damage occurred. A fiber failure was observed at pulse energies exceeding 3.2 mJ with a peak power of 0.35 MW, corresponding to an energy density at the input fiber end-face of 310 Jcm^{-2} and a peak power density of 34.3 $GWcm^{-2}$, which is approximately three times greater than previously achieved for standard HC-PCFs [16]. The input end of the fiber was destroyed and light guidance was no longer observed. The main reason of the fiber failure at this particular pulse energy is a high M^2 value of the laser beam introducing a poorer coupling efficiency (in comparison with the ps laser) and mismatch with the fiber guided-mode, which results in light being partially incident on the fiber cladding and damaging the structure. Therefore, the peak power density at which the damaged occurred is significantly lower than for the ps laser. Due to the lack of an available ns laser with a better beam quality providing sufficient pulse energy it was impossible to determine the energy handling capabilites of the NCF in the ns pulse regime. However, based on the obtained results we think that this fiber can successfully withstand higher pulses energies in both ns and ps pulse regime.

3.2 Nanosecond pulse delivery

To demonstrate the suitability of the fiber-delivered ns pulses for micro-machining applications a diode-pumped Spectra Physics Q-switched Nd:YVO_4 laser (M^2<1.3) was used. The laser operated at 1064 nm providing 60 ns pulses with an energy above 1 mJ (ideal for precision machining applications) and an average power of 18.2 W at a repetition rate of 15 kHz. The pulse delivery tests were conducted for both a 0.7 m fiber without bending and a 10.5 m NCF coiled to a diameter of 60 cm. The laser beam was launched directly into the fiber using a plano-convex lens giving a focused spot diameter of 36 μm ($1/e^2$) with a focus cone angle of 0.03 rad (matching the acceptance angle of the fiber). The high quality of the laser beam presented in Fig. 7(a) and well optimized coupling parameters (for the maximum delivered power) allowed a coupling efficiency of 92% to be obtained. The maximum pulse energy from the laser was coupled into the fiber without damage, providing fiber-delivered

#191496 - $15.00 USD Received 12 Jun 2013; revised 7 Sep 2013; accepted 9 Sep 2013; published 19 Sep 2013

pulses of energy 1.1 mJ with an average power of 16.3 W and a peak power of 18.3 kW. As described in [16], the fiber damage threshold normally scales with $\tau^{0.5}$, where τ is the pulse duration. Thus, given the damage threshold measured for the 9 ns pulses, we would expect the fiber to be capable of delivering at least 8 mJ in a 60 ns pulse before damage occurs. This is approximately 16 times greater than previously achieved with a conventional 7-cell defect HC-PCF [1]. After propagation through 10.5 m of NCF, the delivered energy was reduced to 0.8 mJ, which was still sufficient for micro-machining (see section 4.1). Figure 7(b) presents the fiber-delivered beam profile captured by imaging the end of the fiber with a CCD camera and Spiricon software, which clearly indicates multi-mode guidance in the fiber. The measured $1/e^2$ diameter of the delivered beam was approximately 36 μm.

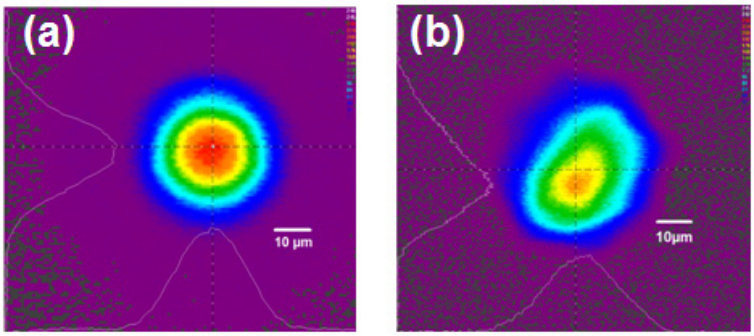

Fig. 7. False-color profiles of: (a) ns laser beam; (b) fiber-delivered beam.

3.3 Picosecond pulse delivery

The experiment was performed using the TRUMPF TruMicro picosecond laser (M^2>1.3) at 1030 nm wavelength, giving 6 ps pulses at 400 kHz repetition rate with a pulse energy of up to 116 μJ and average and peak powers of 46.3 W and 19.3 MW respectively. The beam from this laser was coupled into a 1 m straight length of fiber and an 8 m coiled length (with 23 cm bending diameter). The tight bending of the fiber was essential due to limited working space.

To couple a laser beam directly into the fiber core a singlet lens providing a focused spot diameter of ~36 μm ($1/e^2$) with a focus cone angle of 0.029 rad was used. The obtained coupling efficiency, ~84%, allowed pulse delivery without fiber damage. The launching parameters were optimized to deliver the maximum power. The launch efficiency is decreased in comparison with the ns laser mainly due to lower laser beam quality as shown in Fig. 8(a) and slight mismatch between the focused cone angle and the fiber acceptance angle. The maximum delivered pulse energy through a 1 m length was 92 μJ with an average power of 36.7 W corresponding to peak power of 15.3 MW. The delivered average and peak powers of the ps pulses are 7 and 2 times greater respectively than previously reported in [11]. The additional high bending loss with the 8 m length reduced the transmitted energy to 49 μJ with an average power of 19.6 W and a peak power of 5.6 MW. The fiber output was characterized with a CCD camera together with Spiricon beam profiling software and the Femtochrome FR-103XL autocorrelator. The delivered beam profile with a diameter of 36 μm ($1/e^2$) is presented in Fig. 8(b). The results of the spatial beam quality measurements of the NCF-delivered ps pulses are presented in Figs. 9(a) and 9(b). The M^2 = 1.5 of the delivered beam shown in Fig. 9(a) corresponds to the highest beam quality that can be delivered through the fiber by coupling the light mostly into the fundamental mode. However, due to the multimode behavior of the fiber the typical profile of the delivered beam with an M^2 of 3.2 is presented in Fig. 9(b).

#191496 - $15.00 USD Received 12 Jun 2013; revised 7 Sep 2013; accepted 9 Sep 2013; published 19 Sep 2013

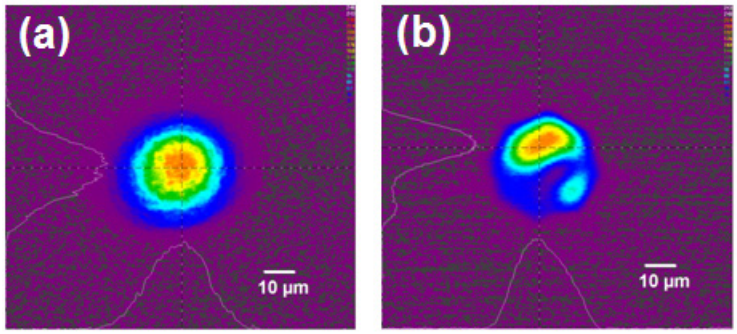

Fig. 8. False-color profiles of: (a) ps laser beam; (b) fiber-delivered beam.

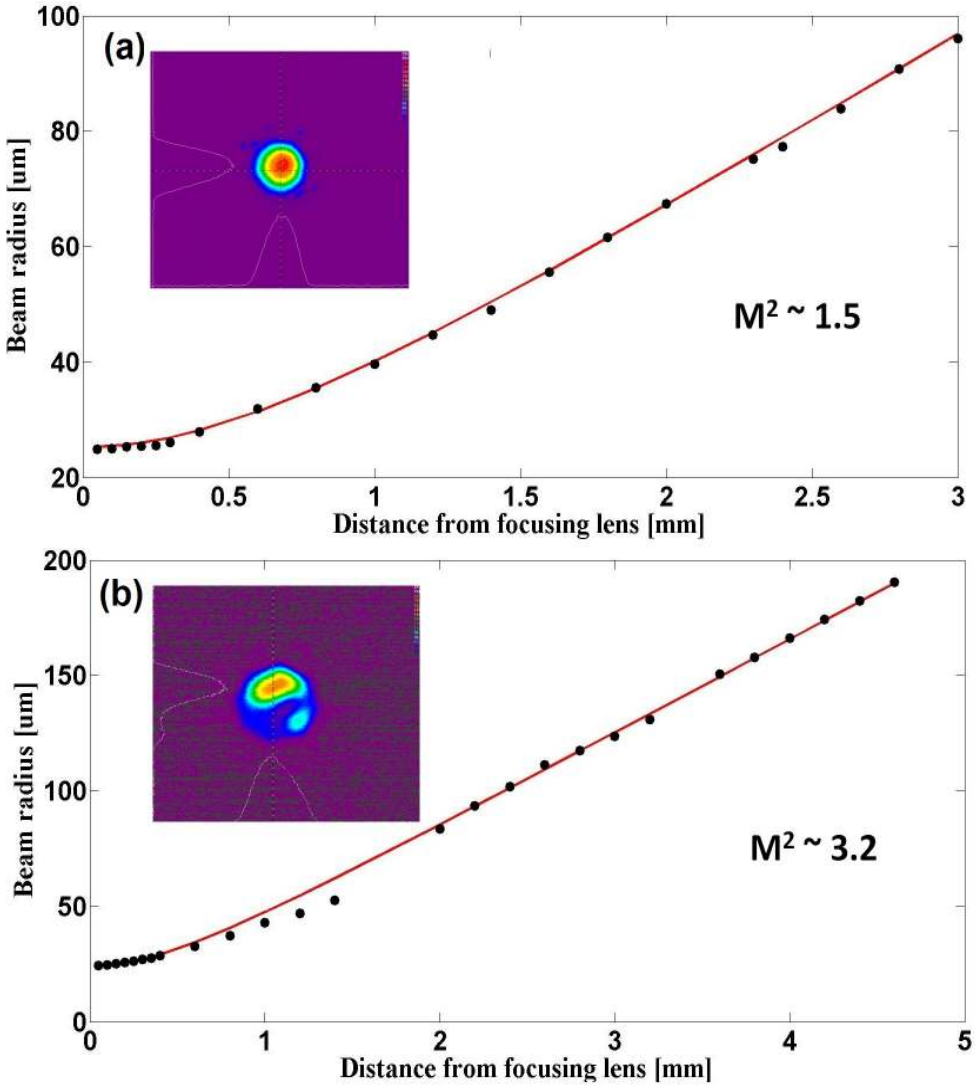

Fig. 9. Results of an M^2 measurements of the NCF-delivered beam for: (a) highest beam quality that can be delivered through the fiber when exciting the fundamental mode; (b) typical beam profile delivered through the fiber.

#191496 - $15.00 USD Received 12 Jun 2013; revised 7 Sep 2013; accepted 9 Sep 2013; published 19 Sep 2013

The intensity autocorrelation of the delivered pulse through 1 m NCF presented in Figs. 10(a) and 10(b) shows no pulse dispersion in comparison with original laser pulse. However, after propagation along 8 m of fiber the transmitted pulse was stretched to 8.7 ps FWHM as plotted in Fig. 10(c), likely to be associated with intermodal dispersion rather than non-linear effects. No significant distortion of the pulse shape was observed. In addition, no measurable degradation between the optical spectra of the laser pulse and NCF-delivered pulse was observed.

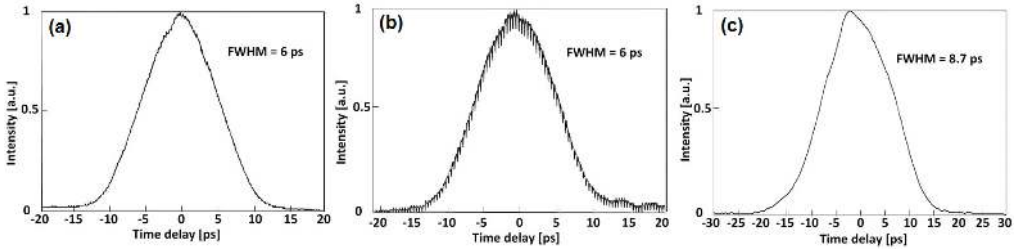

Fig. 10. Intensity autocorrelation of: (a) laser pulse; (b) pulse delivered through 1 m of NCF; (c) pulse transmitted through 8 m of coiled (Ø 23cm) NCF (different scale on time delay axis) .

4. Fiber-delivered light for micro-machining

4.1 Nanosecond and picosecond micro-machining

Suitability of the fiber-delivered laser beam for machining applications was demonstrated by through cutting of aluminum sheet and marking of titanium with the ns laser and milling of fused silica with the ps laser. The experimental setup for fiber-based micro-machining is shown in Fig. 11. The laser-fiber coupling arrangement was identical to that used previously. A half-wave plate and polarizing cube beam splitter were used to provide precise power control without affecting the laser-fiber coupling efficiency. The output of the fiber was collimated with a singlet plano-convex lens and a telescope used to expand the beam to match the entrance aperture (14 mm diameter) of the galvo scan head. The focal lengths of the f-theta lenses in the galvo scan head were 125 mm and 160 mm for the ns and ps lasers respectively. The focused spot diameters at the workpiece were calculated to be approximately 30 μm ($1/e^2$) for the ns laser and 36 μm ($1/e^2$) for the ps laser. The lengths of the NCF used for the machining were 1 m (bent) and 10.5 m (coiled) for the ps and ns lasers respectively.

#191496 - $15.00 USD Received 12 Jun 2013; revised 7 Sep 2013; accepted 9 Sep 2013; published 19 Sep 2013

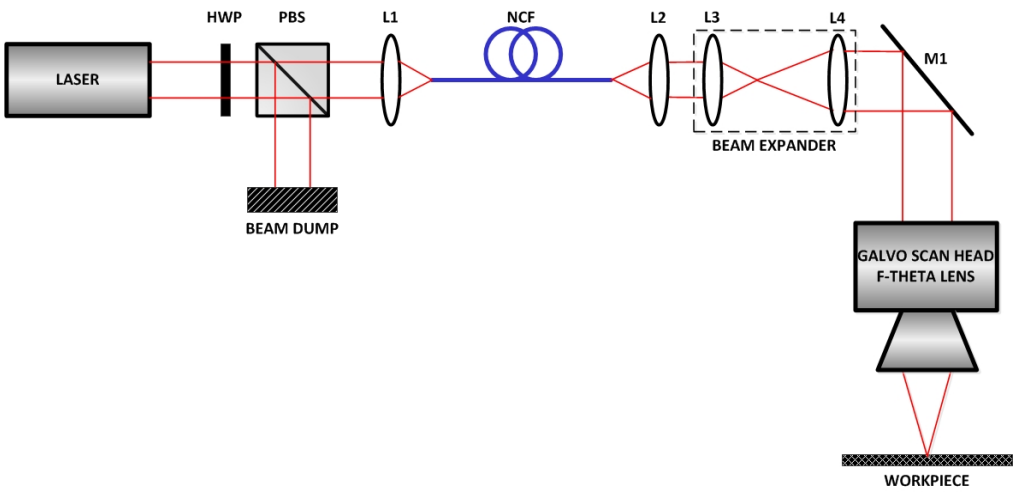

Fig. 11. The experimental setup for ns and ps fiber-based micro-machining. HWP: half-wave plate; PBS: polarizing beam splitter; L: lens; M: mirror.

The 1064 nm, 60 ns laser parameters used for through cutting of the 0.3 mm thick aluminum sheet were 0.8 mJ, pulses at a repetition rate of 15 kHz. The delivered pulse energy was sufficient to perform precise cutting of relatively small shapes, less than 1 mm by 1 mm with a cutting speed of 1 mm/s, see Fig. 12. Despite the multi-mode nature of the fiber and bending-induced profile changes, high quality shapes were generated.

Fig. 12. Example of cutting through of the 0.3 mm thick aluminum sheet with the ns laser.

Marking in titanium was performed using identical machining parameters, but with a significantly higher surface speed of 100 mm/s. To fabricate the features a raster scanning method was used. Excellent results were achieved as shown in Fig. 13. No thermal damage to the surrounding material was observed.

#191496 - $15.00 USD Received 12 Jun 2013; revised 7 Sep 2013; accepted 9 Sep 2013; published 19 Sep 2013

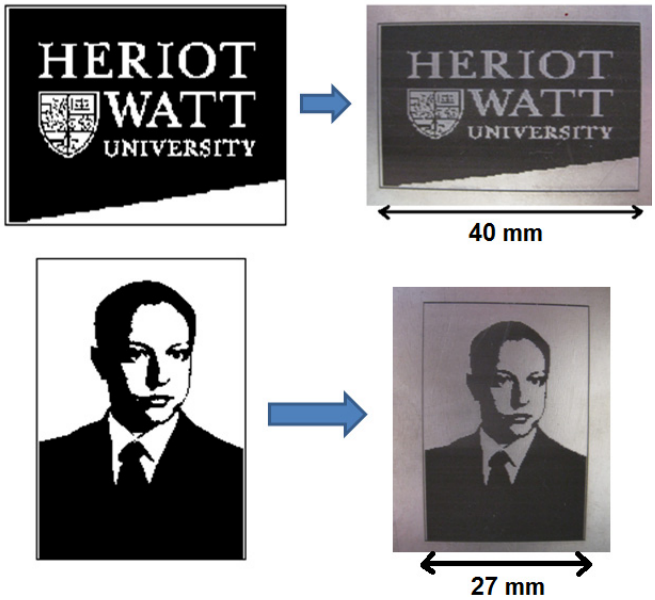

Fig. 13. Examples of ns marking in titanium: source bitmaps (left) and machined patterns (right).

Picosecond fiber-delivered pulses were used to perform high-quality machining of 1.5 mm thick fused silica. With the 1030 nm 6 ps laser, the pulsed energy used for machining was approximately 52 μJ at a 400 kHz repetition rate. The marking speed was set to 100 mm/s. This allowed fabricating features with the dimensions less than 1mm by 1mm with depth of 30 μm. The examples of machined fused silica are shown in Fig. 14. No cracks on the glass structure were observed. To our knowledge this was the first demonstration of a crack-free machining of glass with fiber-delivered ps pulses at 1 μm wavelength region, which is not possible to achieve with solid core LMA and conventional hollow-core fibers due to low damage threshold and non-linear effects in the short pulse regime. Moreover, crack-free milling of fused silica is not possible with longer (ns) pulses (which can be delivered through i.e. solid core LMA fibers) due to thermal effects raised on the glass.

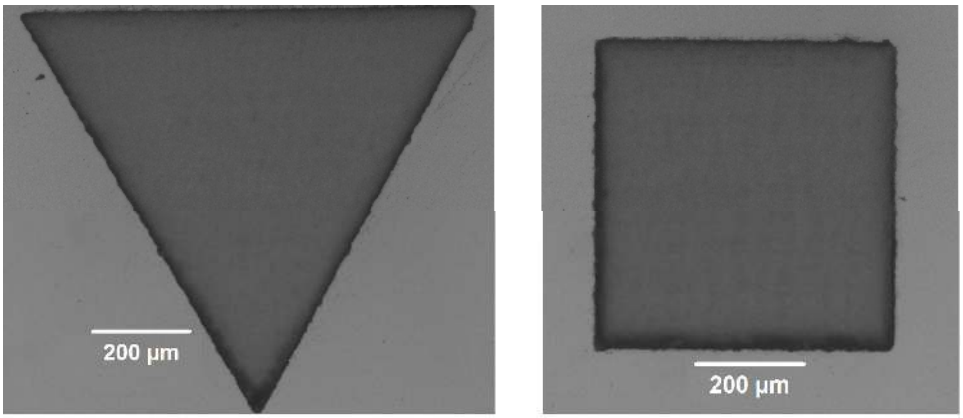

Fig. 14. Micro-milled patterns in fused silica with ps fiber-delivered pulses.

5. Conclusions

In this paper we have presented high-power nanosecond and picosecond pulse delivery through a novel hollow-core Negative Curvature Fiber for micro-machining applications. We

#191496 - $15.00 USD Received 12 Jun 2013; revised 7 Sep 2013; accepted 9 Sep 2013; published 19 Sep 2013

report for the first time successful transmission of ps pulses with an average power more than 36 W, which is 7 times greater than previously reported with a hypocycloid-core kagome-type HC-PCF [11]. The non-complex structure of the fiber, consisting of only a single cladding layer makes it relatively easy to fabricate compared with other ARROW-guiding fiber designs i.e. hypocycloid-core kagome fibers. The energy handling capability of the fiber is significantly higher than for the typical hollow-core photonic crystal fibers and conventional silica fibers. Moreover, it was not possible to establish the ultimate damage threshold due to the lack of a sufficiently powerful laser system, therefore we assume that the NCF can withstand higher pulse energies than reported here. The delivered pulse energies and average powers are of the level required for precision micro-machining applications. High quality machining and marking has been demonstrated, despite the fiber being multi-mode with a somewhat unstable output profile due to its bend-sensitivity which makes the NCF a perfect candidate for a solution to the flexibility problem of high-average power pulsed lasers. Further development of the fiber will focus on modifying its structure to obtain more efficient separation between the cladding nodes and the core to achieve single-mode, low-loss and bend-insensitive high-power beam delivery.

Acknowledgments

This work is funded by the UK Engineering and Physical Sciences Research Council under grants EP/I01246X/1 and EP/I011315/1. The authors would like to thank Renishaw plc for providing additional funding and Christopher Leburn for loaning the autocorrelator and helping with the pulse width measurements.